Low-energy electron collisions with pyrrole

Eliane M. de Oliveira, Marco A. P. Lima, Márcio H. F. Bettega, Sergio d'A. Sanchez, Romarly F. da Costa et al.

Citation: J. Chem. Phys. **132**, 204301 (2010); doi: 10.1063/1.3428620
View online: http://dx.doi.org/10.1063/1.3428620
View Table of Contents: http://jcp.aip.org/resource/1/JCPSA6/v132/i20
Published by the AIP Publishing LLC.

Low-energy electron collisions with pyrrole

Eliane M. de Oliveira,[1] Marco A. P. Lima,[1,2] Márcio H. F. Bettega,[3] Sergio d'A. Sanchez,[3] Romarly F. da Costa,[4] and Márcio T. do N. Varella[4,a)]

[1]*Instituto de Física Gleb Wataghin, Universidade Estadual de Campinas, 13083-970 Campinas, São Paulo, Brazil*

[2]*Laboratório Nacional de Ciência e Tecnologia do Bioetanol (CTBE), Centro Nacional de Pesquisa em Energia e Materiais (CNPEM), 13083-970 Campinas, São Paulo, Brazil*

[3]*Departamento de Física, Universidade Federal do Paraná, Caixa Postal 19044, 81531-990, Curitiba, Paraná, Brazil*

[4]*Centro de Ciências Naturais e Humanas, Universidade Federal do ABC, Rua Santa Adélia, 166, 09210-170 Santo André, São Paulo, Brazil*

(Received 8 March 2010; accepted 21 April 2010; published online 25 May 2010)

We report cross sections for low-energy elastic electron scattering by pyrrole, obtained with the Schwinger multichannel method implemented with pseudopotentials. Our calculations indicate π^* shape resonances in the B_1 and A_2 symmetries, and two σ^* resonances in the A_1 symmetry (the system belongs to the C_{2v} point group). The present assignments of π^* resonances are very close to those previously reported for the isoelectronic furan molecule, in agreement with electron transmission spectra. The lowest-lying σ^* anion is localized on the N–H bond and provides a dissociation coordinate similar to those found in the hydroxyl groups of organic acids and alcohols. This σ^*_{NH} resonance overlaps the higher-lying π^* resonance (possibly both π^* states) and could give rise to direct and indirect dissociation pathways, which arise from electron attachment to σ^* and π^* orbitals, respectively. The photochemistry of pyrrole and 9-H adenine is similar, in particular with respect to the photostability mechanism that allows for the dissipation of the photon energy, and we believe pyrrole would also be a suitable prototype for studies of dissociative electron attachment (DEA) to DNA bases. We point out the connection between the mechanisms of photostability and DEA since both arise from the occupation of σ^* and π^* orbitals in neutral excited states and in anion states, respectively. © *2010 American Institute of Physics*. [doi:10.1063/1.3428620]

I. INTRODUCTION

The discovery[1] that low-energy electrons can induce single- and double-strand breaks in DNA brought considerable attention to electron interactions with molecules of biological relevance.[2] The high-energy radiation employed in radiology and radiotherapy generates a large number of fast electrons in living cells. These electrons thermalize in a picosecond scale,[3] eventually forming metastable anions (resonances) with either the nucleic acid subunits or the surrounding water molecules. Striking experimental evidence that radiation damage could be mediated by dissociative electron attachment (DEA) at low energies was provided by Sanche and co-workers.[1,4,5] These authors observed a resonantlike energy dependence of strand breaks upon irradiation of plasmid DNA with slow electrons, especially for energies between 5 and 15 eV, and this process was subsequently found to occur locally (independently of the long range geometrical structure of DNA). Though it may sound unexpected that low-energy electrons (as opposed to MeV photons) would ultimately be responsible for radiation damage, DEA has long been known a very efficient mechanism of energy transfer into nuclear degrees of freedom.

DNA subunits can attach electrons in either σ^* and π^* orbitals, where long-lived anions are formed in the latter case, and short-lived though dissociative anions in the former case. A direct dissociation mechanism thus arises from the formation of σ^* resonances, while the formation of π^* ions diabatically coupled to σ^* ions gives rise to indirect dissociation pathways. These mechanisms were proposed based on bound-state approximations to resonant states of DNA subunits[6,7] and have been confirmed by scattering calculations for smaller organic molecules.[8–10] An accurate description of the resonant states is computationally demanding since DNA components are considerably large molecules with low symmetry. The vast majority of *ab initio* scattering calculations addressed elastic collisions[11–15] at a single geometry, and little has been learned about the topology of resonant potential energy surfaces.[11] Moreover, model descriptions of the electron-target correlation-polarization potential[11,12] might not always lead to accurate resonance spectra,[16,17] making DEA studies of biomolecules very challenging tasks.

In view of these difficulties, considerable attention has been paid to prototype molecules, such as small organic acids,[8,9,18,19] pyrazine,[20] and furan,[21] which may allow for more detailed studies (in particular, the correlation between resonances and electronic excitation channels[20,22]). This work reports elastic electron scattering by the moderately large and highly symmetric pyrrole molecule, which we

a)Author to whom correspondence should be addressed. Electronic mail: marcio.varella@ufabc.edu.br.

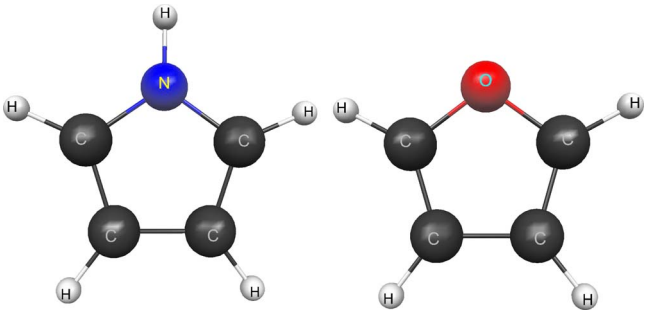

FIG. 1. Geometrical structures of pyrrole (left) and furan (right).

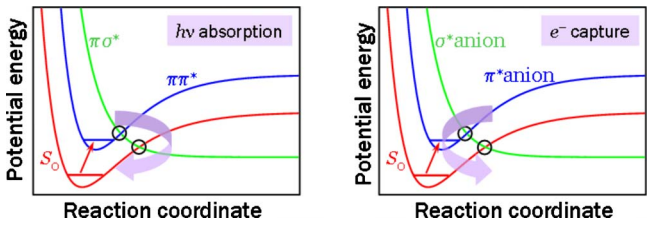

FIG. 2. Schematic representation of the photostability (left) and indirect DEA (right) mechanisms for an arbitrary reaction coordinate. In the left panel, photon absorption excites the molecule to a bright $\pi\pi^*$ state (blue line). The internal conversion mechanism involves diabatic couplings between the $\pi\pi^*$ state and the dissociative $\pi\sigma^*$ state (green), and between the $\pi\sigma^*$ state and the ground state (red line), thus allowing for the dissipation of the photon energy. In the right panel, electron attachment to a π^* orbital gives rise to a long-lived π^* resonance (blue line), diabatically coupled to a dissociative σ^* resonance (green line). The crossing of the latter $(N+1)$-electron resonance potential with the N-electron ground state potential (red line) stabilizes the anion, thus leading to dissociation. The imaginary parts of the resonance potentials are not shown.

believe a suitable prototype for studies of DEA in biomolecules. Though pyrrole is isoelectronic and very similar to furan (see Fig. 1), it has a polar σ(N–H) bond that provides a dissociation channel also found in 9-H adenine. In fact, the photochemistry of pyrrole and 9-H adenine is similar in the sense that $\pi\pi^*/\pi\sigma^*$ and $\pi\sigma^*/S_0$ conical intersections, where S_0 is the ground sate and $\pi\pi^*$ and $\pi\sigma^*$ are excited electronic states, seem to provide protection against photodissociation.[23] The excited $\pi\pi^*$ state is usually bright (optically coupled to the ground state) and diabatically coupled to the dissociative $\pi\sigma^*$ state. The latter is also coupled to the ground state and provides an internal conversion mechanism ($\pi\pi^* \rightarrow \pi\sigma^* \rightarrow S_0$) that converts the photon energy into vibrational energy,[24] preventing the molecule from undergoing photoinduced damage. Since nucleic acid bases strongly absorb radiation in the ultraviolet range, this and other internal conversion channels[25] allow for the nonradiative dissipation of the photon energy into the environment, thus playing a crucial role in the photostability of life.[26]

There is a fascinating connection between the above photostability mechanism and the indirect DEA pathway, which would prevail over the direct mechanism in DNA bases at low energies. Electron attachment to a π^* orbital gives rise to a long-lived resonance diabatically coupled to a dissociative σ^* anion state. The crossing of the latter resonance potential with the ground state potential stabilizes the anion and *leads* to dissociation; while the crossing between the (neutral) $\pi\sigma^*$ excited state with the ground state, in the photoinduced internal conversion pathway, *prevents* dissociation (see Fig. 2). The building blocks of life, though stable against photoabsorption leading to reactive $\pi\pi^*$ states, are unstable against electron attachment to virtual π^* orbitals. We believe comparative studies of photostability and DEA in biomolecules, both driven by the occupation of σ^* and π^* orbitals, have been largely overlooked. This work reports elastic electron scattering by pyrrole at the fixed-nuclei approximation, as a first step toward elaborate studies of dissociation dynamics. We discuss the existence of π^* and σ^* resonances for this system to validate it as a suitable prototype for DEA studies in DNA bases. The resonant states of pyrrole are compared with those of the isoelectronic molecule furan to inspect the signature of σ^* resonances coupled to the N–H dissociation coordinate (absent in the latter).

This paper is organized as follows. The Schwinger multichannel (SMC) method employed in the scattering calculations and the computational procedures are outlined in Secs. II and III, respectively. Our results are presented and discussed in Sec. IV, and the conclusions are summarized in Sec. V.

II. THEORY

Scattering calculations were performed with the SMC (Ref. 27) implemented with the pseudopotentials[28] of Bachelet *et al.*,[29] within the minimal orbital basis for single configuration interaction approximation.[30] The method and its implementation are discussed in detail elsewhere,[27,28,30] and here we only give the working expression for the scattering amplitude

$$f(\mathbf{k}_i,\mathbf{k}_f) = -\frac{1}{2\pi}\sum_{m,n}\langle S_{\mathbf{k}_f}|V|\chi_m\rangle(d^{-1})_{mn}\langle\chi_n|V|S_{\mathbf{k}_i}\rangle, \quad (1)$$

where

$$d_{mn} = \langle\chi_m|A^{(+)}|\chi_n\rangle, \quad (2)$$

and

$$A^{(+)} = \left(\frac{\hat{H}}{N+1} - \frac{\hat{H}P + P\hat{H}}{2} + \frac{PV + VP}{2} - VG_P^{(+)}V\right). \quad (3)$$

In the expressions above, P is a projector onto energy-allowed target electronic channels, $G_P^{(+)}$ is the free-particle Green's function projected onto P space, V is the projectile-target interaction potential, and $\hat{H}=(E-H)$ is the collision energy minus the scattering Hamiltonian given by $H=H_0+V$, where H_0 describes the noninteracting electron-molecule system. $S_{\mathbf{k}}$ is a solution of H_0 and χ_m's are $(N+1)$-particle configuration state functions, given by products of target electronic states and projectile scattering orbitals, which provide the basis set for expansion of the trial scattering wave function. The open electronic collision channels are included in the P space (only the ground state in the present application) and the dynamical response of the target electrons to the projectile field (polarization effects) are accounted for through virtual excitations of the target.

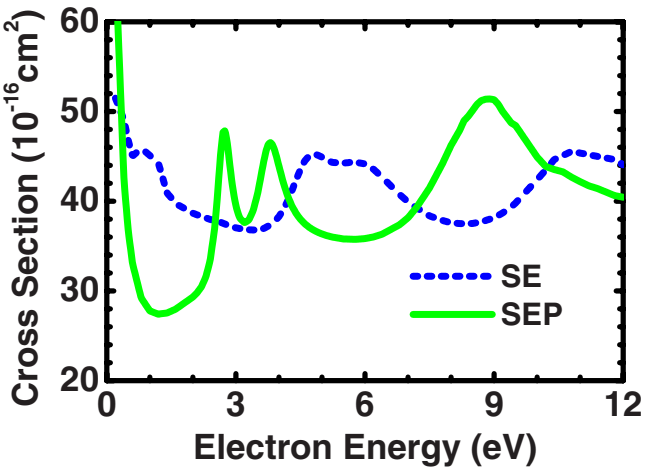

FIG. 3. ICS for electron scattering by pyrrole, obtained with the SE (broken line) and SEP (full line) approximations. The peak around 8.7 eV in SEP calculations has contributions from physical and unphysical structures (see text).

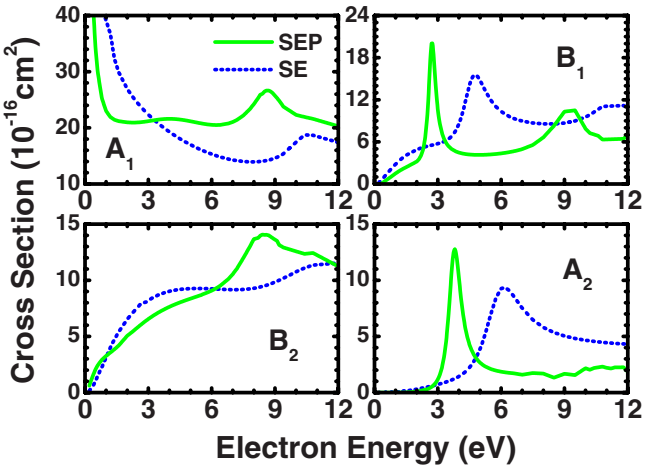

FIG. 4. Symmetry decomposition of the electron-pyrrole ICS obtained with the SE (broken lines) and SEP (full lines) approximations.

III. COMPUTATIONAL PROCEDURES

The target electronic ground state was described at the restricted Hartree–Fock (HF) level with $5s5p2d$ Cartesian Gaussian basis sets on the carbon and nitrogen atoms and a $3s$ basis set on the hydrogen atoms. The basis of the hydrogen atom bonded to nitrogen was further augmented with a $2s1p$ set of diffuse atomic orbitals chosen in an even tempered fashion (successively dividing the exponents by 3.0) to account for the $3s$ Rydberg character of the lowest σ^* orbital.[23] (Convergence tests employing a different basis set were also carried out.) The HF equilibrium geometry shown in Fig. 1 was obtained with the GAMESS package[31] employing the 6-311++G(d,p) basis set, with the target treated as a C_{2v} molecule. Though the computed dipole moment of 1.895 D is in good agreement with the experimental value of 1.84 D, the scattering cross sections were not corrected to account for the long-range dipole interaction because we are mainly interested in obtaining the spectrum of shape resonances. Both target and scattering calculations employed the local-density norm-conserving pseudopotentials of Bachelet, Hamann, and Schlüter[29] (BHS) to represent the nuclei and the $1s$ core electrons of carbon and nitrogen (details of the implementation of the BHS pseudopotentials in the HF and SMC methods are given elsewhere[28]).

Our calculations were carried out in the static-exchange (SE) and static-exchange-plus-polarization (SEP) approximations, where correlation-polarization effects are accounted for in the latter. The closed-channel space comprised all singlet- and triplet-coupled single-particle excitations from the valence orbitals to a set of modified virtual orbitals (MVOs) (Ref. 32) lying below a suitably chosen energy cutoff (−15.0 eV), and these MVOs were also used as scattering orbitals (a closed-shell cationic Fock operator with charge +4 was employed to generate the MVOs). For the totally symmetric A_1 irreducible representation an additional set of polarized orbitals,[33] generated from the MVOs lying above the energy cutoff, were used as both particle and scattering orbitals, amounting to a total of 7824 configurations to expand the scattering wave function in this symmetry. We expect this combination of MVOs and polarized orbitals to account for short-range correlation and long-range polarization effects, thus properly describing the A_1 resonances and the large background (see below). For the other symmetries, the total number of configurations was 2192 (B_1), 2463 (B_2), and 2132 (A_2).

IV. RESULTS AND DISCUSSION

The elastic integral cross section (ICS) for electron-pyrrole scattering is shown in Fig. 3, and its symmetry decomposition is presented in Fig. 4. The SE calculations show π^* resonances in both the B_1 (4.8 eV) and A_2 (6.2 eV) symmetries, and these are shifted to lower energies in SEP calculations, as expected, to 2.7 and 3.8 eV, respectively. A σ^* shape resonance is clearly observed in the A_1 symmetry around 10.4 eV (SE) and 8.7 eV (SEP), and a broad structure is found in the B_1 symmetry around 12.5 eV (SE) and 8.4 eV (SEP). The peak around 9.0 eV in the B_1 symmetry is likely spurious, arising from open electronic channels treated as closed in the present elastic approximation, so the large peak around 8.5–9.0 eV in the ICS would have both physical and unphysical contributions. The present assignments of π^* resonances are in good agreement though overestimated with respect to electron transmission (ET) measurements,[34] as shown in Table I. For the B_1 and A_2 symmetries, we also performed scattering calculations employing a single MVO as a scattering orbital, as proposed elsewhere[35] to provide a

TABLE I. Resonance peak positions obtained from SMC cross sections, in units of eV. Also shown are the VAEs reported by Modelli and Burrow (Ref. 34). VAE_{exp} are ET experimental results; VAE_{MP2} and VAE_{B3LYP} are theoretical predictions based on VO energies calculated with MP2/6-31G* and B3LYP/6-31G* approximations, respectively.

	SMC	VAE_{MP2}	VAE_{B3LYP}	VAE_{exp}
$\pi^*_{b_1}$	2.7	2.11	2.33	2.36
$\pi^*_{a_2}$	3.8	3.17	3.33	3.45
σ^*_{NH}	4.0	2.93[a]	⋯	⋯
σ^*_{ring}	8.7	4.52[a]	⋯	⋯

[a]Estimates obtained from VO energies reported in Ref. 34 and the C–Cl σ^* linear scaling of Ref. 36.

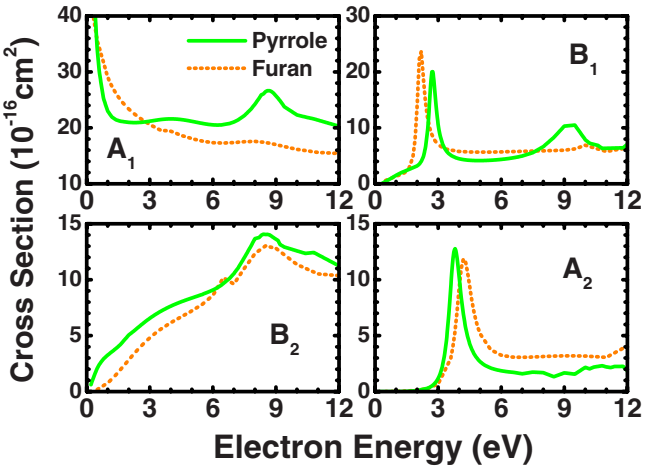

FIG. 5. Partial cross sections for electron scattering by pyrrole (full line) and furan (broken line).

balanced description of polarization effects, and the agreement with ET results was slightly worse. We also believe the broad peak around 4.0 eV in the A_1 partial cross section would also be a σ^* resonance located on the N–H bond, as discussed below.

The SEP partial cross sections of pyrrole are compared with those of furan in Fig. 5. As expected, there is great similarity in the π^* resonance spectra, though the furan B_1 peak lies 0.6 eV below its pyrrole counterpart. This is consistent with experimental data in the sense that π^* vertical attachment energy (VAE) assignments for both molecules are equal within the resolution of ET spectra.[34] The higher σ^* resonance of pyrrole (8.7 eV in the A_1 symmetry) does not have a clear signature in furan, though a smooth structure around 8.0 eV is found in the latter. As shown in Fig. 6, the most significant difference in the differential cross sections is observed around 7.5 eV since pyrrole displays a *d*-wave behavior not seen in furan. We believe this oscillation arises from the σ^* resonance at 8.7 eV since the *d*-wave character is stronger at this energy.

Though subtle, the most interesting difference between these isoelectronic molecules is perhaps the broad peak

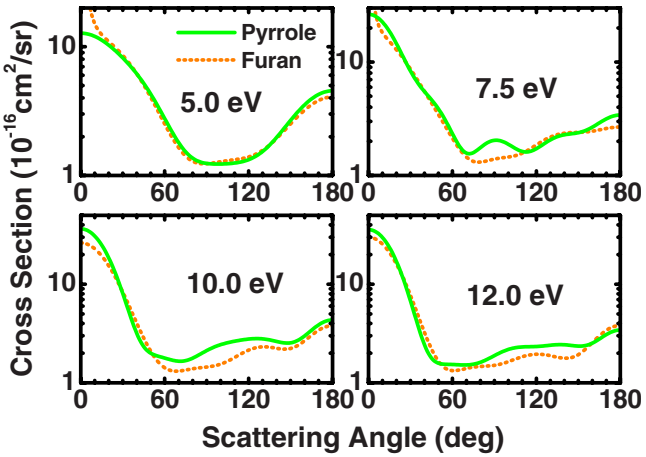

FIG. 6. Differential cross sections for electron scattering by pyrrole (full line) and furan (broken line). The calculations were not corrected to account for the long-range dipole interaction.

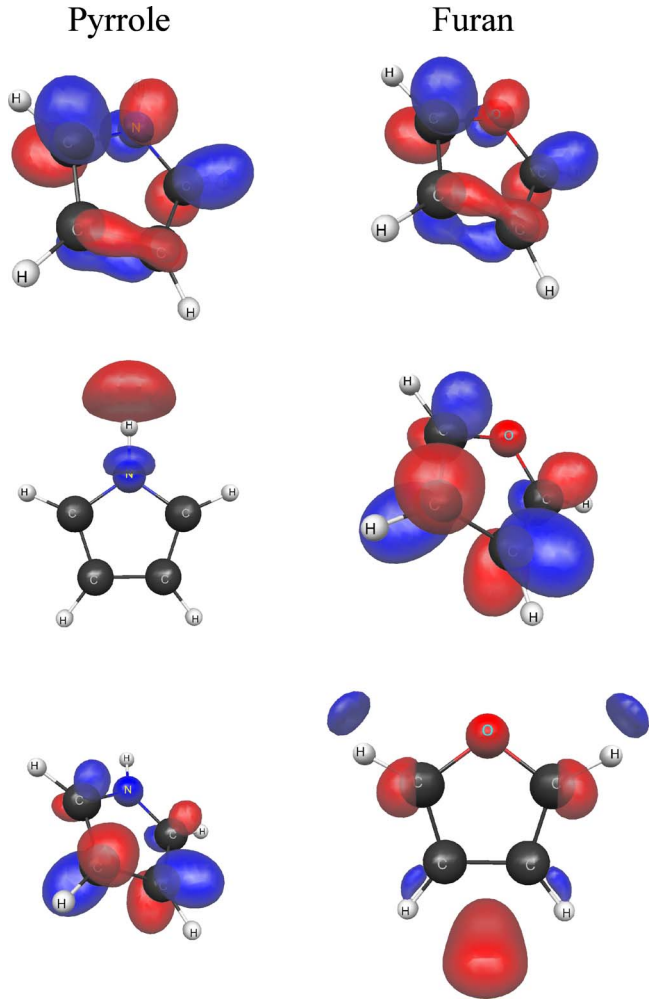

FIG. 7. Left panel: lowest VOs of pyrrole. From top to bottom LUMO ($\pi^*_{b_1}$), LUMO+1 ($\sigma^*_{a_1}$), and LUMO+2 ($\pi^*_{a_2}$). Right panel: lowest VOs of furan. From top to bottom LUMO ($\pi^*_{b_1}$), LUMO+1 ($\pi^*_{a_2}$), and LUMO+2 ($\sigma^*_{a_1}$).

around 4.0 eV in the A_1 partial cross section of pyrrole (Fig. 5), which is absent in furan. To gain further insight into resonance characters, we performed bound state calculations at the HF level, employing minimal basis sets. The lowest unoccupied orbitals, namely LUMO, LUMO+1, and LUMO+2 (LUMO denotes lowest unoccupied molecular orbital), of pyrrole and furan are represented in Fig. 7. In pyrrole, these are $\pi^*_4(b_1)$, $\sigma^*_7(a_1)$, and $\pi^*_5(a_2)$, while $\pi^*_4(b_1)$, $\pi^*_5(a_2)$, and $\sigma^*_7(a_1)$ in furan. $\sigma^*(a_1)$ virtual orbitals (VOs) strongly localized on the N–H bond and lying below the $\pi^*_5(a_2)$ VOs were also obtained from MP2/6-31G* and B3LYP/6-31G* calculations reported by Modelli and Burrow,[34] and these authors speculated on the existence of a broad σ^*_{NH} resonance which would be masked in the ET spectrum by the more intense signal of the A_2 π^* anion. Though care should be taken in assigning a broad resonance embedded in a large background, we believe such σ^*_{NH} resonance does exist and has a reasonably clear signature in the $l=2$ partial wave. Exploratory calculations also indicated that the structure moves to the left (right) and becomes narrower (broader) as the N–H bond is stretched (shortened). From the MP2/6-31G* VO energy of Ref. 34, the σ^*_{NH} VAE can be

predicted to lie around 2.9 eV, with the help of the empirical linear scaling relation reported elsewhere[36] for C–Cl σ^* resonances. Though significantly underestimated with respect to the present value of 4.0 eV, this result would be reasonable in the sense that scaling of σ^* VO energies has not been extensively investigated.[34] In fact, formic acid has a broad σ^*_{OH} resonance with VAE around 4.5 eV (Ref. 9) and application of the above scaling relation to the lowest σ^* VO leads to a VAE of 2.9 eV.[37] These values are remarkably close to those of the σ^*_{NH} pyrrole resonance, suggesting a general feature arising from localization on the polar bond. It should be mentioned, however, that direct observation of the σ^*_{NH} resonance in total or elastic ICS measurements would be challenging since it could be masked by the long-range dipole interaction neglected in the present calculations.

In view of the polar character of the N–H bond, the σ^*_{NH} resonance would be expected to give rise to DEA, in much the same way as σ^*_{OH} anions of organic acids[9,37] and alcohols.[38] The existence of such broad dissociative resonance overlapping the A_2 π^* state, if not both π^* anions, could in principle give rise to both direct and indirect dissociation pathways. In this sense, the pyrrole molecule would be validated as a suitable prototype for studies of DEA in biomolecules, and the conjecture that photostability and indirect DEA go along each other (Fig. 2) would be supported by the present results (taking into account the photochemistry of pyrrole[23]). In formic acid, the DEA peak for the $[HCOOH]^- \rightarrow HCOO^- + H$ reaction lies nearly 0.5 eV below the π^* VAE, and would result from direct attachment to the higher-lying broad σ^*_{OH} resonance.[9,37] From the gas-phase acidity of pyrrole [1504 kJ/mol (Ref. 39)] the DEA onset for hydrogen atom release would be around 1.98 eV, close to the B_1 π^* resonance VAE of 2.36 eV (Table I). It is thus not certain if the prevailing DEA mechanism around 2.0–2.5 eV would be the direct pathway found in carboxyl moieties or the indirect mechanism observed in DNA bases, whose DEA onsets are on top of π^* VAEs.[40] At higher energies, around 3.5–4.0 eV, competition between attachment to the σ^*_{NH} or the A_2 π^* resonance would be expected, though the electronic excitation threshold around 4.2 eV (Ref. 41) would open up core-excited channels, making the collision dynamics much more complex.[20,22,42]

V. CONCLUSIONS

We have reported cross sections for elastic electron scattering by pyrrole. Our SEP calculations indicate a rich resonance spectrum comprising B_1 π^* (2.7 eV), A_2 π^* (3.8 eV), A_1 σ^*_{NH} (4.0 eV), and A_1 σ^*_{ring} (8.7 eV) anion states. The present π^* assignments are in good agreement with ET measurements and are very similar to those of the isoelectronic furan molecule. Though not shown here, the LUMO+5 orbital of pyrrole, which is the second VO in the A_1 symmetry, is very similar to the LUMO+2 orbital of furan, shown in Fig. 7, though with higher probability around the heteroatom in pyrrole. Despite this similarity, pyrrole displays a strong σ^* shape resonance around 8.7 eV, which is not as clear in furan (a smooth broad structure is found around 8.0 eV, though). The existence of a σ^*_{NH} resonance in pyrrole was previously considered based on the VO spectrum,[34] and was confirmed by the present calculations. This dissociative broad resonance overlaps at least the higher-lying π^* state, if not both π^* states, and would thus give rise to direct and indirect dissociation pathways, though we cannot come to a conclusion about the prevailing hydrogen elimination mechanism based on the present fixed-nuclei calculations. These results corroborate pyrrole as a suitable prototype for DEA studies in DNA bases and points out the connection between the mechanisms of electron-driven dissociation and photostability, since these arise from the occupation of σ^* and π^* orbitals in anion states and in neutral excited states, respectively.

ACKNOWLEDGMENTS

E.M.O. acknowledges a fellowship from Coordenação de Aperfeiçoamento de Pessoal de Nível Superior (CAPES). S.d'A.S. and R.F.daC. acknowledge fellowships from Fundação de Amparo à Pesquisa do Estado de São Paulo (FAPESP). M.A.P.L., M.H.F.B., and M.T.N.V. acknowledge research grants from Conselho Nacional de Desenvolvimento Científico e Tecnológico (CNPq). M.H.F.B. also acknowledges support from FINEP (CT-Infra project) and from Fundação Araucária, as well as computational support from Professor Carlos de Carvalho at DFis-UFPR and from Professor Carlos de Carvalho and Professor Wagner Zola at LCPAD-UFPR. This work is supported by the CNPq/NSF Cooperative Research Program, and by the FAPESP Bioenergy Program (BIOEN). The present calculations were partly performed at Centro Nacional de Processamento de Alto Desempenho (CENAPAD-SP).

[1] B. Boudaïffa, P. Cloutier, D. Hunting, M. A. Huels, and L. Sanche, Science **287**, 1658 (2000).
[2] For a review, see: L. Sanche, Eur. Phys. J. D **35**, 367 (2005).
[3] S. Gohlke and E. Illenberger, Europhys. News **33**, 207 (2002).
[4] M. A. Huels, B. Boudaïffa, P. Cloutier, D. Hunting, and L. Sanche, J. Am. Chem. Soc. **125**, 4467 (2003).
[5] F. Martin, P. D. Burrow, Z. Cai, P. Cloutier, D. Hunting, and L. Sanche, Phys. Rev. Lett. **93**, 068101 (2004).
[6] I. Anusiewicz, M. Sobczyk, J. Berdys-Kochanska, P. Skurski, and J. Simons, J. Phys. Chem. A **109**, 484 (2005) (and references therein).
[7] J. Gu, Y. Xie, and H. F. Schaefer III, J. Am. Chem. Soc. **127**, 1053 (2005).
[8] T. N. Rescigno, C. S. Trevisan, and A. E. Orel, Phys. Rev. Lett. **96**, 213201 (2006); Phys. Rev. A **80**, 046701 (2009).
[9] G. A. Gallup, P. D. Burrow, and I. I. Fabrikant, Phys. Rev. A **79**, 042701 (2009); Phys. Rev. A **80**, 046702 (2009).
[10] T. P. M. Goumans, F. A. Gianturco, F. Sebastianelli, I. Baccarelli, and J. L. Rivail, J. Chem. Theory Comput. **5**, 217 (2009).
[11] F. A. Gianturco and R. R. Lucchese, J. Chem. Phys. **120**, 7446 (2004); F. A. Gianturco, F. Sebastianelli, R. R. Lucchese, I. Baccarelli, and N. Sanna, *ibid.* **128**, 174302 (2008).
[12] I. Baccarelli, F. A. Gianturco, A. Grandi, N. Sanna, R. R. Lucchese, I. Bald, J. Kopyra, and E. Illenberger, J. Am. Chem. Soc. **129**, 6269 (2007).
[13] S. Tonzani and C. H. Greene, J. Chem. Phys. **124**, 054312 (2006); J. Chem. Phys. **124**, 094504 (2006).
[14] C. Winstead, V. McKoy, and S. d'A. Sanchez, J. Chem. Phys. **127**, 085105 (2007).
[15] C. Winstead and V. McKoy, J. Chem. Phys. **125**, 244302 (2006); J. Chem. Phys. **125**, 074302 (2006).
[16] P. D. Burrow, J. Chem. Phys. **122**, 087105 (2005).
[17] C. Winstead and V. McKoy, J. Chem. Phys. **129**, 077101 (2008).
[18] M. H. F. Bettega, Phys. Rev. A **74**, 054701 (2006); T. C. Freitas, M. T. do N. Varella, R. F. da Costa, M. A. P. Lima, and M. H. F. Bettega, *ibid.* **79**,

022706 (2009).
[19] F. A. Gianturco, R. R. Lucchese, J. Langer, I. Martin, M. Stano, G. Karwasz, and E. Illenberger, Eur. Phys. J. D **35**, 417 (2005); F. A. Gianturco and R. R. Lucchese, *ibid.* **39**, 399 (2006).
[20] C. Winstead and V. McKoy, Phys. Rev. Lett. **98**, 113201 (2007); Phys. Rev. A **76**, 012712 (2007).
[21] M. H. F. Bettega and M. A. P. Lima, J. Chem. Phys. **126**, 194317 (2007).
[22] R. F. da Costa, M. H. F. Bettega, and M. A. P. Lima, Phys. Rev. A **77**, 012717 (2008).
[23] A. L. Sobolewski,W. Domcke, C. Dedonder-Lardeux, and C. Jouvet, Phys. Chem. Chem. Phys. **4**, 1093 (2002).
[24] H. Satzger, D. Townsend, M. Z. Zgierski, S. Patchkovskii, S. Ullrich, and A. Stolow, Proc. Natl. Acad. Sci. U.S.A. **103**, 10196 (2006).
[25] S. Perun, A. L. Sobolewski, and W. Domcke, J. Am. Chem. Soc. **127**, 6257 (2005).
[26] A. L. Sobolewski and W. Domcke, Europhys. News **37**, 20 (2006).
[27] K. Takatsuka and V. McKoy, Phys. Rev. A. **24**, 2437 (1981); Phys. Rev. A **30**, 1734 (1984).
[28] M. H. F. Bettega, L. G. Ferreira, and M. A. P. Lima, Phys. Rev. A **47**, 1111 (1993).
[29] G. B. Bachelet, D. R. Hamann, and M. Schlüter, Phys. Rev. B **26**, 4199 (1982).
[30] R. F. da Costa, F. J. da Paixão, and M. A. P. Lima, J. Phys. B **37**, L129 (2004).
[31] M. W. Schmidt, K. K. Baldridge, J. A. Boatz, S. T. Elbert, M. S. Gordon, J. H. Jensen, S. Koseki, N. Matsunaga, K. A. Nguyen, S. J. Su, T. L. Windus, M. Dupuis, and J. A. Montgomery, J. Comput. Chem. **14**, 1347 (1993).
[32] C. W. Bauschlicher, Jr., J. Chem. Phys. **72**, 880 (1980).
[33] W. Sun, C. W. McCurdy, and B. H. Lengsfield III, J. Chem. Phys. **97**, 5480 (1992); T. N. Rescigno, A. E. Orel, and C. W. McCurdy, Phys. Rev. A **56**, 2855 (1997).
[34] A. Modelli and P. W. Burrow, J. Phys. Chem. A **108**, 5721 (2004).
[35] C. Winstead and V. McKoy, Phys. Rev. A **57**, 3589 (1998).
[36] K. Aflatooni, G. A. Gallup, and P. D. Burrow, J. Phys. Chem. A **104**, 7359 (2000).
[37] A. M. Scheer, P. Mozejko, G. A. Gallup, and P. D. Burrow, J. Chem. Phys. **126**, 174301 (2007).
[38] B. C. Ibănescu, O. May, A. Monney, and M. Allan, Phys. Chem. Chem. Phys. **9**, 3163 (2007).
[39] NIST Chemistry webbook, http://webbook.nist.gov/chemistry.
[40] K. Aflatooni, A. M. Scheer, and P. D. Burrow, J. Chem. Phys. **125**, 054301 (2006).
[41] B. O. Roos, L. Serrano-Andrés, and M. Merchán, Pure Appl. Chem. **65**, 1693 (1993).
[42] R. F. da Costa, M. H. F. Bettega, and M. A. P. Lima, Phys. Rev. A **77**, 042723 (2008).